Binding of Sulfate Terminated Surfactants with Different Alkyl Chain Lengths to Viologen Sites Covalently Embedded in the Interior of a Self-Assembled Monolayer on a Au Electrode

Takamasa Sagara*,†, Youichi Hagi‡, Masaki Toyohara§

†Division of Chemistry and Materials Science, Graduate School of Engineering, Nagasaki University, Nagasaki, Nagasaki 852-8121, Japan

‡Department of Materials Engineering and Molecular Science, Graduate School of Science and Technology, Nagasaki University, Bunkyo 1-14, Nagasaki 852-8521, Japan

§Department of Advanced Technology and Science for Sustainable Development, Graduate School of Engineering, Nagasaki University, Nagasaki, 852-8521, Japan

KEYWORDS: *viologen thiol, self-assembled monolayer, alkyl sulfate, electrostatic binding, chain-chain interaction, Traube rule*

ABSTRACT: Although much has become well-known about the structures and properties of redox-active self-assembled monolayers (SAMs) on electrode surfaces, their uses as electro-active platforms are still under development. Interaction of the SAM with foreign molecules such as amphiphiles in the solution phase brings about new functionalities. We focused on the enhancement of the redox-dependent binding of anionic surfactants to the cationic redox-active site attached to an alkyl-thiol molecule that forms a SAM on a poly-crystalline Au electrode. There are two main points. One is that we embedded a viologen site in the midway of the alkyl chain to facilitate ion-pairing in the micro-environment of a low dielectric constant. The other is the use of alkyl chain-chain interaction as an important mode of attraction between the surfactants and SAM. We found in the SAM with viologen sites located midway that the binding of anionic surfactants and inorganic anions causes a negative shift of the formal potential of the redox couple of viologen radical cation/viologen dication in line with the binding equilibrium. In contrast, the anion binding is weak and trivial when viologens are located at the SAM surface. For the SAM with viologens located midway, the surfactant chain-length dependent shift of the formal potential was clearly observed; it followed the Traube rule but with a smaller slope than that in the original rule. The strong binding enabled us to discuss the blocking and electron transfer mediation abilities of the Au/viologen-SAM/dodecyl sulfate adlayer.

INTRODUCTION

Fine control and enhancement of specific interaction between surfactants and a self-assembled monolayer (SAM) have significant impacts on the fabrication of the platforms of electrochemical devices. One typical application is the sensing and determination of surfactants in aqueous solutions. Another aspect is the construction of an electro-active functional molecular assembly involving surfactants. In this paper, we focus on the interaction of anionic surfactants to an electroactive-cationic SAM.

The behavior of anionic surfactants at aqueous electrified interfaces at lower concentrations than their critical micelle concentrations (*cmc*) was investigated by tensiometry at a Hg electrode in 1950-70. The direct adsorption of an ionic surfactant on a bare Hg electrode surface[1] was subjected to electrocapillary measurements to obtain the interfacial tension as a function of the concentration. The surface tension change of a Hg drop electrode occurs by adsorption and adlayer formation of the surfactants with complicated multiple phase changes of the adlayer.[2,3] Since the 1990s, organized structures of surfactant molecules directly adsorbed on well-defined solid electrode surfaces were clarified at a molecular level. Typical structures of dodecyl sulfate anion (DS^-) on Au(111) electrodes include a hemi-micellar adlayer and an interdigitated bilayer.[4-10]

Because of the amphiphilicity, ionic surfactants in an aqueous solution exhibit specific interaction with organic monolayers on electrode surfaces. On an alkanethiol SAM on a Au electrode in water, ionic surfactant forms a second overlayer on the SAM below or near *cmc*. The main factor is the chain-chain interaction, as demonstrated by interfacial differential capacity as a function of the concentration of surfactants such as tetradecanoic acid and dodecylpyridinium chloride.[11] The structures of the surfactant molecules on both a SAM with a terminal cationic site and an alkanethiol SAM were discussed using the results of the force measurements by atomic force microscope (AFM).[12] Cui *et al.* demonstrated patching of pinholes in a sub-monolayer of

octadecanethiol on an Au electrode by DS^- from aqueous solution,[13] and Bandyopadhyay *et al.* reported the properties of adlayers formed from mixed solutions of a sulfate terminated surfactant and an alkanethiol.[14]

Redox-active SAMs have also been used to explore their interaction with surfactants. The most typical one is the SAM of a ferrocene (Fc)-terminated alkyl thiol (FC-SAM). The strong binding of soft inorganic anions to the oxidatively generated terminal ferrocenium cation (Fc^+) was first reported by Uosaki *et al.*[15] They described the Nernstian shift of redox potential of Fc/Fc^+ couple as a function of the concentration of the anions. Later, the ion-pair binding of ClO_4^- to the terminal Fc^+ site was supported by electrochemical frequency-modulated AFM.[16] The ion-pair formation with various anions has been extensively discussed.[17-20]

Detailed studies of the ion-pair formation of the Fc^+ terminal group with alkyl sulfate surfactants in a wide concentration range have been made. Norman and Badia found in 2007 that DS^- undergoes specific ion-pair formation with the electrochemically induced Fc^+ as the surface group of a Fc-SAM.[21] Dionne and Badia extensively investigated the ion-pair formation of various anionic surfactants at the surface of the Fc-SAM in a wide range of surfactant concentrations at least over one order of magnitude higher and lower than the *cmc*.[22] They established dependence of the redox potential of Fc/Fc^+ couple on the chain length of the surfactants. However, the mechanism behind the dependence was unclear, because the Fc sites at the SAM surface are always exposed to the solution phase. Therefore, in the case of Fc-SAM with terminal Fc sites, electrostatic attraction works between the Fc sites and anionic surfactant molecules, no matter whether monomeric or micellar, while the chain-chain interaction works only between surfactant molecules.

In contrast to the FC-SAM, because a viologen unit has two substituents at both ends of a 4,4'-pyridinium, we can embed viologen sites in the interior of the SAM. We may locate the sites not too deep from the water phase to allow the penetration of the anionic head group to reach the viologen and simultaneously to effect electrostatic attraction by providing a lower dielectric constant microenvironment for the viologen site. This can enhance the electrostatic binding of the anion head group to the viologen cations. Both the oxidized forms, viologen dication (V^{2+}), and the one-electron reduced form, viologen monocation mono-radical ($V^{\bullet+}$), are cationic and therefore interact electrostatically with anions.

In this work, we aimed to enhance the interaction of anionic surfactants from the bulk of aqueous solution to the viologen thiol-SAM (VT-SAM) on a Au electrode. To make the viologen location dependence clear, we used two viologen thiols as the precursor of the SAM. Namely, one has only a methyl group at the outer side of viologen (**MeVC10-SH**), while the other has a heptyl chain (**C7VC10-SH**) (Figure 1). We used cyclic voltammograms (CVs) and the results of the measurements of X-ray photoelectron spectroscopy (XPS) and electroreflectance (ER) spectroscopy to describe the interaction of DS^- and some other anionic surfactants with the viologen-SAMs on a poly-crystalline Au (poly-Au) electrode. Of particular, we focused on (i) the effect of the location of the binding of anion head with viologen cation in the low

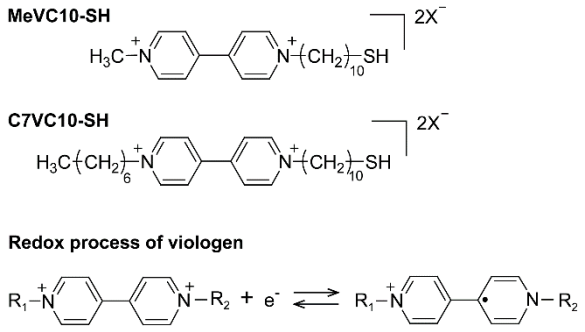

Figure 1. Molecular structures and redox process of viologen.

dielectric constant micro-environment and (ii) the discriminative evaluation of the interaction between surfactant-chain and SAM-chain. We showed the merit that we have the always-cationic site in the midway of the alkyl chain in the VT-SAM of **C7VC10-SH**. The low dielectric environment in the alkyl phase should enhance the electrostatic interaction. Because Au crystals exposing specific facets have not been used frequently as a substrate of the devices in mass-production and because a recent report pointed out the complexity in the VT-SAM formation on a Au(1 1 1) terrace[23], we used a poly-Au electrode. It would be intriguing to see the difference between poly-Au and single-crystalline Au as the substrates, but we will report this topic in a separate paper.

Electrostatic interaction of viologens with organic anions bearing a long alkyl chain drives the formation of a self-assembling structure. In the micelle-like complexes of sodium-DS^- and a fluorophore, the fluorescence was quenched by V^{2+} even below *cmc*.[24] The effects of interaction between viologen and anionic surfactants, such as DS^-, on the viologen electrochemistry have been investigated.[25-28] Especially, strong binding of viologens to a DS^- micelle is well known.[29] Viologen also acts as a template to induce aggregation of anionic polymers.[30] When a cationic viologen bearing a long hydrophobic chain interacts with an anionic surfactant in an aqueous medium, both electrostatic and chain-chain interactions play predominant roles in their binding processes.[31, 32]

The redox potential of $V^{\bullet+}/V^{2+}$ couple of VT-SAM is more negative in the presence of more hydrophobic anions because of stronger binding to V^{2+}[33, 34]. The difference between the potential with ClO_4^- and that with Cl^- is smaller when the viologen moiety is more exposed to the solution phase.[35] The structure of the VT-SAM on a crystalline Au electrode surface and its interaction with anions have been reported by the group of Wandlowski.[36-38] Wen *et al.* have recently synthesized several VT with a viologen moiety located in the midway of the alkyl chain to estimate the electric field strength as a function of the distance from the electrode surface.[39] The longitudinal axis of viologen in the SAM was largely tilted from the surface normal of the electrode as revealed by the ER measurements[40-42] by us and STM and IR measurements by Li *et al.* [36] These features allow our evaluation of the binding of alkyl sulfate to VT-SAM and discrimination between electrostatic and interchain interactions.

In this work, we pay close attention to the binding of the head group of an anionic surfactant to the embedded viologen in the alkyl phase of the VT-SAM. We evaluate the work required to transfer an alkyl chain of a surfactant monomer in an aqueous solution to the interior of the SAM. We also shed light on the location dependence, midway or terminal, and the properties of the film formed with the surfactants.

EXPERIMENTAL SECTION

N-heptyl-*N'*-(10-mercapto)decyl-4,4'-bipyridinium (**C7VC10-SH**) and *N*-methyl-*N'*-(10-mercapto)decyl-4,4'-bipyridinium (**MeVC10-SH**) salts were synthesized in our laboratory. All the other chemicals were of reagent grade and were used without further purification. Water was purified through a Milli-Q integral (Millipore) to a resistivity > 18 MΩ cm. A poly-Au disk electrode with a geometric surface area of 0.020 cm^2 (BAS) was polished with a 0.3 μm and then a 0.05 μm alumina slurry to a mirror finish and then rinsed in water. After the treatment of the Au electrode by oxidation-reduction cycle in 0.01 M $HClO_4$, the SAM formation of **C7VC10-SH** as a PF_6^- or Br^- salt was made by dipping the poly-Au electrode in 0.5 or 1 mM acetonitrile or ethanolic solution of the VT for 24 h in the dark at room temperature. The electrode was then rinsed by the same solvent and subsequently by water. The SAM formation of **MeVC10-SH** was made by dipping the polished electrode in a 10 mM **MeVC10-SH** salt + tris(2-carboxyethyl)phosphine (TCEP) solution in methanol + water (7:3 vol/vol) for 24 h. After rinsing, the Au electrode with the SAM was placed in the cell filled with the deaerated aqueous electrolyte solution. An Ag/AgCl electrode in saturated KCl solution was used as the reference electrode. A coiled Au wire served as the counter electrode. All the measurements were carried out in an argon gas (>99.998%) atmosphere at 23 ± 2°C.

The potential modulation used for electroreflectance (ER) measurements is described as

$$E = E_{dc} + E_{ac} = E_{dc} + \Delta E_{ac} \exp(j\omega t) \quad (1)$$

where E_{dc} is the dc potential, E_{ac} is the ac potential, ΔE_{ac} is the zero-to-peak ac amplitude of the potential modulation, $j = \sqrt{-1}$, and $\omega = 2\pi f$ where f is the modulation frequency. The instruments and procedures used for the ER measurements were described in our previous paper[41] and chapter[42].

RESULTS AND DISCUSSION

Characterization of Au/C7VC10-SH-SAM. A VT-SAM of **C7VC10-SH** on a poly-Au electrode was first used to uncover the binding of anions, alkyl sulfates, and alkyl benzene sulfonates with different chain lengths, to the VT-SAM at lower concentrations than *cmc*. Our surface tension measurements confirmed that the *cmc* of SDS + 0.1 M KF solution is higher than 7×10^{-4} M, being consistent with the values reported by Dionne and Badia for SDS + 0.3 M NaF (*cmc* = 1.1 mM).[22] Our measurements also found that hexadecyl sulfate up to 1×10^{-4} M in 0.05 M KF gives a solution of monomer only.

First, the **C7VC10-SH**-SAM with counter anions of PF_6^- or Br^- was subjected to multiple cyclic scans of the electrode potential (E) in 0.10 M KF solution until the redox response reached a steady-state CV. After a typical steady-state CV (curve a in Figure 2) was obtained, XPS measurements were made for the electrode taken out from the solution followed by rinsing with water (Table S1). The results revealed that PF_6^- or Br^- initially present in the VT-SAM were exchanged completely for F^- through repeated redox interconversion between V^{2+} and $V^{\bullet+}$.

The CV obtained for the Au/VT(F^-)-SAM electrode (curve a) showed characteristics that the peak currents are proportional to the potential sweep rate, the peak potentials are constant at the weep rates lower than 0.2 V s^{-1} with non-zero peak separation, and the peaks are wider than the width for the reversible wave of the Langmuir adsorption layer. The response is of a quasi-reversible redox reaction of the VT monolayer with a formal potential, $E^{o\prime}$, for $V^{2+}/V^{\bullet+}$ couple at -301 mV, irrespective of the KF concentration. The non-ideality of the width originates likely from the repulsive interaction between viologen sites, and the peak potential separation comes from the conformation change of the VT molecules upon the redox.

Then, the Au/VT(F^-)-SAM electrode was transferred to the solution containing 300 μM SDS. The CV (curve b in Figure 2) showed significantly more negative anodic and cathodic peak potentials than those obtained in KF solutions. The sharper peak shape and narrower peak separation than those in KF solutions indicate anion binding to the viologen site to weaken the inter-site repulsion and suppress the conformation change.[34,41] XPS measurements for the electrode after the CV measurements in SDS solution showed increased content of carbon atoms (Table S1), indicating the binding of DS^- to the VT-SAM. We found that electrostatic attraction is a prerequisite of the binding, because (i) a neutral surfactant, dodecyl hexaoxymethylene glycol monoether gave ca. 10 mV positive shift regardless of the concentration around 300 μM, and (ii) quaternary ammonium-type cationic surfactants showed no effect.

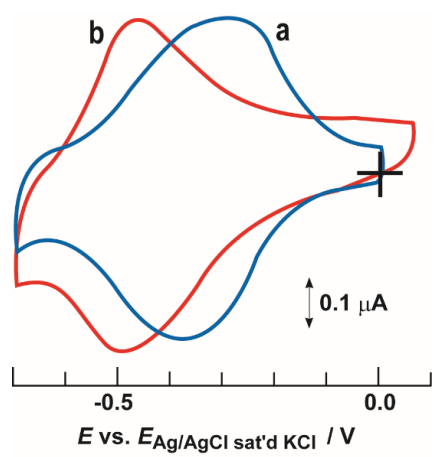

Figure 2. A steady state CV (curve **a**) of **Au/C7VC10-SH**-SAM at 100 mV s^{-1} reached after repeated potential cycling in 0.10 M KF solution at 23°C. Curve **b**: CV in 300 μM SDS + 0.1 M KF solution.

The CVs of the Au/VT-SAM electrode showed proportionality of the peak current to the potential sweep rate, indicative of the thin-layer redox reaction of the $V^{\bullet+}/V^{2+}$ couple shown in Figure 1. The superficial amount of active viologen, Γ, obtained from the charge under the peak ranged from 2.0 to 3.6 × 10^{-10} mol cm^{-2} due to sample-to-sample deviation because of the use of polished poly-Au without correction of surface area for the surface roughness. The average was Γ= 3.0 × 10^{-10} mol cm^{-2}. Provided that all VT molecules in the SAM are electro-active, the value of Γ represents the saturated amount of immobilized VT molecules. This amount is ca. 40% of that for an alkanethiol monolayer.

The obtained ER spectra were of the type of the difference absorption spectral waveform irrespective of the solution composition (Figure S1). The reduced form, $V^{\bullet+}$, tends to dimerize to be $V^{\bullet+}$-dimer. The ER spectrum demonstrated that, when viologens are reduced to $V^{\bullet+}$, more than 60 % of them form $V^{\bullet+}$-dimer. The dependence of the ER signal intensity with *p*-polarized incident light relative to that with *s*-polarized light was obtained as a function of the incident angle of the light. It revealed that the longitudinal axis of $V^{\bullet+}$ assumes 55-70° oblique orientation with respect to the surface normal.

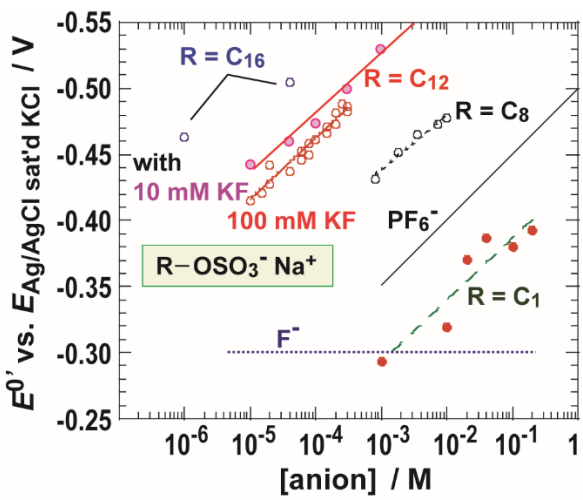

Figure 3. The plot of the formal potential, $E^{o\prime}$, of $V^{\bullet+}/V^{2+}$ couple in Au/**C7VC10-SH**-SAM as a function of anion concentrations. The concentrations of electrolyte KF, c_{KF}, are given in Table 1. For R = C12 (SDS), both c_{KF} = 100 mM and 10 mM were used.

Figure 3 shows the plots of formal potential, $E^{o\prime}$, obtained from the CVs at various concentrations of alkyl sulfates. The value of $E^{o\prime}$ was equated to the midpoint potential between anodic and cathodic peaks of CV at the extrapolated zero-sweep rate. We previously described $E^{o\prime}$ as a function of anion concentration $[A^-]$:[41]

$$E^{o\prime} = E^{o} + \frac{RT}{n_a F} ln \frac{1+K_{red}[A^-]}{1+K_{ox}[A^-]^2} \quad (2)$$

where E^o is the standard redox potential of $V^{2+}/V^{\bullet+}$ couple, n_a is the apparent number of electrons involved in the redox equilibrium, R is the gas constant, F is the Faraday constant, T is the temperature, and K_{ox} and K_{red} are the binding equilibrium constants describing the processes:

$$V^{2+} + 2A^- = V^{2+}...2A^- \qquad K_{ox}$$

$$V^{\bullet+} + A^- = V^{\bullet+}...A^- \qquad K_{red}$$

When the anion binding is so strong that $K_{red}[A^-] >> 1$ and $K_{ox}[A^-]^2 >> 1$, we can rewrite:

$$E^{o'} = E_1 - \frac{RT}{n_a F} \ln \frac{K_{ox}}{K_{red}} - \frac{RT}{n_a F} \ln[A^-] \quad (3)$$

where E_1 is the value of $E^{o\prime}$ at the weak binding limit, being equal to E^o.

E_1 is equated to the $E^{o\prime}$ value in KF solutions, because we definitely had a region of KF concentration (c_{KF}) in which $E^{o\prime}$ is independent of c_{KF} as shown in Figure 3. The plot for the case of PF_6^- is shown as the black solid straight line. The SDS concentration dependence of $E^{o\prime}$ with a slope of 45.4 mV/decade is in line with the last term of Eq. (3), with a value of n_a = 1.29. A negative shift of $E^{o\prime}$ with increasing the chain length is obvious. The surfactant anions bind to the VT-SAM at V^{2+} sites more strongly than at $V^{\bullet+}$ site, while the ratio of the binding equilibrium constant is independent of the anion concentration.

In this work, KF was added when necessary to lower the uncompensated solution resistance. Dionne and Badia showed that the $E^{o\prime}$-surfactant concentration relationship is not largely affected by the addition of 0.3 M NaF below the surfactants' *cmc* for the ferrocene-thiol SAM when decyl and dodecyl sulfates were used.[22] The parallel shift of the plot in Figure 3 by lowering c_{KF} from 100 mM to 10 mM corresponds to a 1.8-fold increase of K_{ox}/K_{red} of DS^-, but it does not change the order of the magnitude of K_{ox}/K_{red}. Such a change was not observed for PF_6^- ion,[41] which has smaller K_{ox}/K_{red} than DS^-. Therefore, the competitive binding of F^- and DS^- is negligible. Most likely, KF shows a weak but detectable electrostatic shielding effect, diminishing the binding of DS^- to the V^{2+} site.

The value of Γ of **C7VC10-SH**-SAM on the Au electrode was unchanged in the presence of any alkyl sulfate and alkyl benzene sulfonate. The alkyl chain domain of the VT-SAM has enough space to allow additional insertion of alkyl chains of the surfactant molecules from the solution phase. Although PF_6^- is more hydrophobic than sulfonate group, the presence of an ethyl benzene group resulted in greater K_{ox}/K_{red} than PF_6^- (Table 1). When the alkyl chain length being up to 8, sulfate surfactants showed a greater K_{ox}/K_{red} than benzene sulfate, whereas with a dodecyl chain, benzene sulfate showed a greater value. The relative amount of carbon atoms in XPS measurements revealed a nearly 1:2 binding ratio of a $[V^{2+}]$:$[DS^-]$ at maximum, indicative of binding of the sulfate head group with the viologen moiety (both

V^{2+} and $V^{\bullet+}$) accompanied by the penetration of at least the part of the alkyl chain. (Table S1).

Table 1. The ratio of K_{ox}/K_{red} obtained using Eq. (3).

anion [a]	K_{ox}/K_{red} (M^{-1})	c_{KF} (mM)
CH_3-OSO_3^-	5.0×10^3	-
PF_6^-	1.2×10^4	100
$CH_3(CH_2)_7OSO_3^-$	1.5×10^6	-
$CH_3(CH_2)_{11}OSO_3^-$	3.0×10^7	100
$CH_3(CH_2)_{15}OSO_3^-$	ca. 2×10^9	50
C_6H_5-SO_3^-	2.1×10^3	-
CH_3CH_2-$(C_6H_4)SO_3^-$	2.6×10^4	10
$CH_3(CH_2)_7$-$(C_6H_4)SO_3^-$	1.0×10^6	10
$CH_3(CH_2)_{11}$-$(C_6H_4)SO_3^-$	$>1.2 \times 10^9$	10

[a] $(C_6H_4)SO_3^-$ stands for a *p*-benzene sulfonate group.

Characterization of Au/MeVC10-SH-SAM. In contrast to the **C7VC10-SH**-SAM, the viologen site of the **MeVC10-SH**-SAM is highly exposed to the aqueous solution phase. Therefore, **MeVC10-SH**-SAM is a suitable reference to unveil the oxidation state dependent interaction between the **C7VC10-SH**-SAM and anionic surfactants. CVs of the Au/**MeVC10-SH**-SAM electrode were sensitive to the SDS concentration in the range from 0.01 to 1 mM but to much less extent than **C7VC10-SH**-SAM. The negative shift of $E^{o\prime}$ was only 20 mV/decade with increasing SDS concentration, although n_a should be nearly unity. In the light of Eq. (2) representing $E^{o\prime}$ before strong bind approximation, if the binding interaction becomes weaker, the slope becomes smaller and asymptotic to zero. The experimental results indicate very weak binding of DS^- to the viologen site of the **MeVC10-SH**-SAM. We also tested the dependence of $E^{o\prime}$ on the concentration of inorganic small anions such as F^-, Cl^-, Br^-, and PF_6^-. Although a shift of $E^{o\prime}$ was observed, no dependence in line with the softness of anions was observed. The insensitivity of **MeVC10-SH**-SAM to the anions was unchanged even though the SAM was formed from the PF_6^- salt of **MeVC10-SH** in acetonitrile, indicating that the insensitivity is an intrinsic property.

The cause of the difference between the behavior of the SAMs of **C7VC10-SH** and **MeVC10-SH** should be the difference in the dielectric micro-environment of the viologen site. The site in the **C7VC10-SH**-SAM was deeply embedded in the low-dielectric medium with a smaller amount of water molecules, whereas that in the **MeVC10-SH**-SAM is well exposed to the water-rich environment and experiences a high-dielectric environment almost the same as in water. This weakens the electrostatic interaction of the viologen site and anions. In the **C7VC10-SH**-SAM, upon the binding of the anionic head group to the viologen site, an alkyl chain of a surfactant inevitably comes in close contact with the alkyl chain of the SAM. The synergy of electrostatic and chain-chain interaction strengthens the binding of anionic surfactant to the **C7VC10-SH**-SAM.

In addition, we found a clear tendency to have smaller immobilized amounts of **MeVC10-SH**; the saturated amount ranged $\Gamma = 1.2 - 2.5 \times 10^{-10}$ mol cm^{-2}. Most likely, the electrostatic repulsion among the terminal V^{2+} sites in the **MeVC10-SH**-SAM formation process resulted in disorder and the greater area occupied by one **MeVC10-SH** molecule than that by **C7VC10-SH** despite the smaller whole molecular size of **MeVC10-SH**.

Dependence on chain length of alkyl sulfate. For all alkyl sulfates, $E^{o\prime}$–ln[A^-] plots for the **C7VC10-SH**-SAM gave straight lines almost parallel to each other (Figure 3). Eq. (3) representing the difference of anion binding equilibrium between V^{2+} and $V^{\bullet+}$, allowed us to obtain $K_G = K_{ox}/K_{red}$ and n_a. As shown in Table 1, a sulfate with a longer alkyl chain has a greater value of K_G. Using

$$K_{ox} = [V^{2+}\ldots 2A^-]/[V^{2+}][A^-]^2 \quad (4)$$

and

$$K_{red} = [V^{\bullet+}\ldots A^-]/[V^{\bullet+}][A^-] \quad (5)$$

we can write the apparent equilibrium represented by K_G on the basis of the Hess's law, keeping in mind that [A^-] is the solution concentration of monomeric A^-:

$$V^{2+} + (V^{\bullet+}\ldots A^-) + A^-(\text{in solution}) = (V^{2+}\ldots 2A^-) + V^{\bullet+} \quad (6)$$

as illustrated in Figure 4.

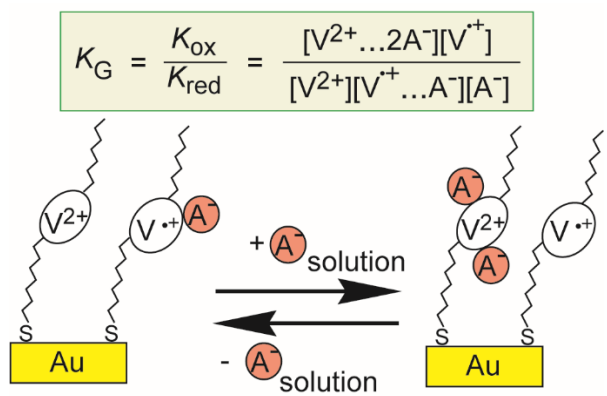

Figure 4. A model to describe the elemental processes in the equilibrium represented by Eq. (6). Alkyl chain of A^- is abbreviated.

The interconversion of the states in Eq. (6) involves two elemental steps:

Step 1: Release of one A^- from $V^{\bullet+}\ldots A^-$ to bind it to V^{2+}. This process takes place in the SAM.

Step 2: Incorporation of one solution-phase A^- from outside into the SAM to bind it to V^{2+}.

Therefore, for the first approximation, the standard Gibbs energy change of the entire process of interest, $\Delta G_t = -RT\ln K_G$, is the sum of ΔG_{es} and ΔG_{in}, where ΔG_{es} is the electrostatic binding energy difference between "$V^{\bullet+}$…anionic site (*i.e.* sulfate group) of alkyl sulfate anion" and "V^{2+}…2 of sulfate groups of alkyl sulfate anion", and ΔG_{in} is the energy to bring an alkyl sulfate from the solution phase into the SAM and to bind it to V^{2+}. The alkyl chain length-dependent energy term is exclusively involved in ΔG_{in}, because new chain-chain interaction is introduced only when the chain of A^- was brought from outside of the SAM.

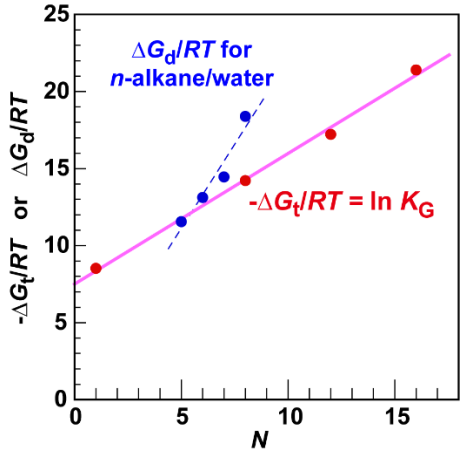

Figure 5. A plot of -ln K_G as a function of N, the number of carbons in the alkyl tail of four alkyl sulfates (red closed circles). The blue broken line shows the Gibbs energy change for alkane molecules with the number of carbons N to be dissolved in water.

As shown in Figure 5, the plot of $\Delta G_t/RT$ as a function of the alkyl chain length gave a straight line with a slope of $0.85RT$ per increment of one $-CH_2-$ group. The intercept was $7.5RT$. These results enabled us to estimate $\Delta G_{in}/N$ = -2.08 kJ mol^{-1} and ΔG_{es} = -18.4 kJ mol^{-1} at experimental temperature (296 K), where N is the number of carbons in the alkyl chain. Provided that ΔG_{es} corresponds to electrostatic interaction between two electronic charges of a distance of 1 nm, the relative dielectric constant of the medium should be 2.30, connoting that the viologens have a place in the low-dielectric micro-environment. Because the experiments were made below *cmc,* ΔG_{in} is a measure of the energy to bring an alkyl chain dissolved in water into the outer alkyl chain layer of the **C7VC10-SH**-SAM.

In Figure 5, the Gibbs energy values of the dissolution process (ΔG_d) of a few liquid alkanes divided by RT are added. The values of ΔG_d were obtained from the molar fractions of saturated alkane aqueous solutions at 25 °C.[43] The ΔG_t-N line has a smaller slope than the ΔG_d-N line shown by a broken straight line. This fact indicates that the outer alkyl chain layer of the **C7VC10-SH**-SAM is less close-packed than liquid alkanes. The results of ER measurements for a **C7VC10-SH**-SAM using polarized incident light revealed that the tilted orientation of the longitudinal axis of viologen moiety from the surface normal by 60-65°, regardless of the concentrations of alkyl sulfate ions (Figure S1). The insertion of alkyl sulfate in the SAM did not affect the SAM structure underneath viologen moieties.

The present results can be compared with the Traube rule.[44-46] This empirical rule originally says that, for a Gibbs layer of alcohols bearing alkyl chains at a gas/water interface, the chain-chain interaction energy corresponding to the transfer from solution phase to the Gibbs layer is ca. 2.68 kJ mol^{-1} per one $-CH_2-$ group. The value was obtained from the surface pressure-N relationship by Traube[44] and re-evaluated by Langmuir[45]. But this value has been reassessed that it is in fact the case that alkyl chains are lying flat on a water surface.[46] Fujimoto *et al.* calculated the energy gain of a normal alkane longer than C2 to be inserted in the alkyl phase of SDS micelle and obtained 3.3 kJ mol^{-1} per one CH_2 group following the Traube rule-like linearity.[47] Wishnia obtained almost the same value, 3.2 kJ mol^{-1} , using the author's own experimental data.[48]

The corresponding value obtained in this work 2.08 kJ mol^{-1} is ca. 60-80% of that in the reported Traube rule values (2.6-3.3 kJ mol^{-1}). The superficial concentration of **C7VC10-SH** at the Au electrode surface was 3.0 × 10^{-10} mol cm^{-2}. Most likely, even when two DS^- binds to one viologen site, the alkyl chain density is still less than the close-packed normal alkyl chains. Note that the chain-chain interaction exceeds the electrostatic interaction when N > 9.

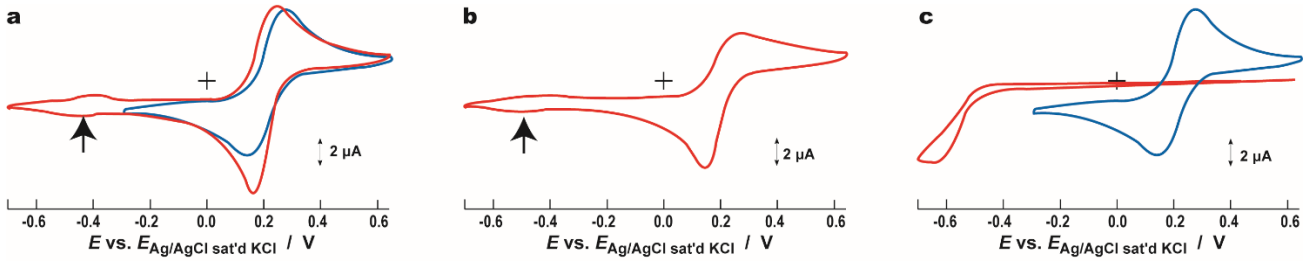

Figure 6. CVs of the Au electrodes covered with **C7VC10-SH**-SAM (red lines) and a bare Au electrode (blue lines) in the solution containing 1.6 mM potassium hexacyanoferrate(III) and 50 mM KF. (a) In the absence of SDS, (b) in the presence of 35 μM SDS, and (c) in the presence of 350 μM SDS. For all the curves, E was swept at 100 mV s^{-1} from the initial potential at the positive end. The black thick arrows mark the redox response of viologen, and the cross points to the zero-current zero-potential origin.

Figure 6 demonstrates the electron transfer (ET) blocking or mediation properties of the DS^- layer on a **C7VC10-SH**-SAM. The **C7VC10-SH**-SAM slightly enhances the redox reaction of $Fe(CN)_6^{4-/3-}$ in the solution phase compared with the reaction at a bare Au electrode (Figure 6-a). No additional cathodic current originated from the mediated ET by the viologen site was observed around $E^{0\prime}$, because the surface concentration of $Fe(CN)_6^{3-}$ was already depleted through reduction. The **C7VC10-SH**-SAM does not act as a blocking layer to suppress the direct ET between Au and the Fe complex. In addition, the positively charged V^{2+} electrostatically attracts anionic $Fe(CN)_6^{3-}$, because F^- does not bind strongly to viologen, leaving the positively-charged viologen site naked and exposed to the solution.

The addition of a low concentration of DS^- in the solution phase decreased the redox peak current of direct ET of the iron complex (Figure 6-b) and increased the peak separation, indicating that the surface-bound DS^- partly neutralizes the positive charge of viologen and increases the density or thickness of the alkyl phase. But the concentration of 35 μM is not enough to block the ET.

With 350 μM of DS^- in the solution phase (Figure 6-c), the adlayer of DS^- appears defect-less and thick enough to block the direct ET completely. Simultaneously, the viologen site mediates the reduction of $Fe(CN)_6^{3-}$ at the reduction potential of viologen. This concentration of SDS is still far below its *cmc.* Interestingly, the negative shift of $E^{0\prime}$ was still observed at higher concentrations of SDS (Figure 3), indicating that 350 μM of DS^- is not necessarily high enough to saturate the binding of DS^- to the **C7VC10-SH**-SAM.

Taken together, with higher concentrations of SDS but still being lower than *cmc*, an interdigitated bilayer of DS^- is formed, similarly to that at a bare Au(111)[4,6,8], on the VT-SAM where the anionic head sulfate groups of the first DS^- layer are strongly bound to the viologen cations in the VT-SAM interior. Because the increase in anionic surfactant concentration did not induce any new voltammetric peak but the shift of $E^{0\prime}$, the formation of another fragmented domain as observed in a Fc-SAM[49] did not occur. The large value of K_{ox}/K_{red} ratio should bring about the modulation of the binary component layered structure by the redox of viologen. Further studies by electrochemical STM and in-situ quartz crystal microbalance may disclose the dynamic structure of the film.

CONCLUSIONS

In the interaction of a redox-active SAM with alkyl sulfate surfactant anions, if once ion pairing between the cationic redox site and the anionic head group(s) of the surfactant is established in the interior of the SAM owing to the low dielectric constant micro-environment, additional chain-chain interaction works obviously. We uncovered the interaction and discussed the natures of the surfactant conjugated-SAM. The results may impact the design of the redox-active sensing platforms that exhibit the oxidation state-driven switching of the binary component molecular assemblies.

We have quantified the contributions of both electrostatic and interchain interactions to the binding of anionic surfactants to the viologen moiety in a viologen-SAM. In sharp contrast to the oxidized state of ferrocene-terminated alkyl thiol SAM, the location of the viologen unit at the midway of the alkyl chain appeared as the determining factor to ensure the strong thermodynamically straightforward binding behavior. To enhance the anion binding to the viologen site in the SAM, the viologen site should be embedded in the low dielectric constant region. The **MeVC10-SH** SAM does not show clear binding behavior, because its viologen site is highly exposed to the aqueous solution.

The dependence of the chain-chain interaction energy in the total interaction energy upon the chain length of alkyl sulfate follows the Traube rule-like behavior but with a much smaller energy slope. Most likely, the full coverage of the **C7VC10-SH** layer is determined by the steric factor of the viologen units, leaving a less-dense alkyl phase than the layer with a full packing of alkyl chains.

We formed VT-SAM from a molecule with a sterically bulky viologen unit on a polished poly-Au surface. Therefore, the inhomogeneity of the SAM structure is inevitable.[50] Nevertheless, the potential shifts in response to the anionic surfactants were highly reproducible. Although we further need to see the molecular-level structure of viologen-thiol SAMs on a Au(111), the present work demonstrated that a conjugated layer of viologen-thiol and anionic surfactant provides us with a new class of versatile interfacial ultrathin films as well as with a highly sensitive interface to the surfactants. The VT-SAM serves as the effective platform for the second layer composed of anionic surfactant and as a functionalized platform of a sensor.

■ ASSOCIATED CONTENT

Supporting Information.
The Supporting Information is available free of charge at http://pubs.acs.org.

Supporting Information. Results of XPS elemental analysis, Results of electroreflectance (ER) measurements (PDF)

■ AUTHOR INFORMATION

Corresponding Author

* **Takamasa Sagara** – Division of Chemistry and Materials Science, Graduate School of Engineering, Nagasaki University, Nagasaki, Nagasaki 852-8121, Japan; ID orcid.org/0000-0002-7975-394X; Email: sagara@nagasaki-u.ac.jp

Authors

Youichi Hagi - Department of Materials Engineering and Molecular Science, Graduate School of Science and Technology, Nagasaki University, Bunkyo 1-14, Nagasaki 852-8521, Japan.

Masaki Toyohara - Department of Advanced Technology and Science for Sustainable Development, Graduate School of Engineering, Nagasaki University, Bunkyo 1-14, Nagasaki, 852-8521, Japan; ID orcid.org/0000-0001-7971-6252

Author Contributions

The concept was led by T.S., and all authors conceived the methodology, measurement system, and experiments. Y.H and M.T. performed the experiments and all authors did the analysis of the data. All authors discussed results, interpreted data. The paper was written mainly by T.S., and all authors approved the submitted version of the manuscript.

Funding Sources

This work was financially supported by a Grant-in-Aid for Scientific Research B (No. 16350077 for TS) from MEXT of Japan Government.

Notes

The authors declare no competing financial interest.

■ ACKNOWLEDGMENT

The authors express their sincere thanks to Mr. Hiroshi Furukawa for his technical assistance for XPS measurements and Mr. Hiroyuki Shiotsuki for his experimental supports. This work was supported in part by MEXT of Japan KAKENHI (grant No. 16350077 for TS).

■ REFERENCES

(1) Součková, J.; Skopalová, J.; Műller; L.; Vymětalíková, M.; Barták, P. A novel fused-silica capillary dropping mercury electrode with long drop-time and its application on determination of critical micelle concentration, *Talanta* **2011**, *84*, 187-191.

(2) Eda, K. Structure of adsorbed layers at the interface of mercury-surfactant solution. III. Structure of adsorbed layers of sodium decyl, dodecyl, and tetradecyl Sulfate. *Nippon Kagaku Zasshi* **1959**, *80*, 349–352.

(3) Eda, K.; Takahashi, K. Structure of adsorbed layers at the interface mercury-surfactant solution. X. Study of the competitive adsorption of two surfactants by the method of differential double layer capacity. *Nippon Kagaku Zasshi* **1964**, *85*, 828–832.

(4) Burgess, I.; Jeffrey, C. A.; Cai, X.; Szymanski, G.; Galus, Z.; J. Lipkowski, Direct visualization of the potential-controlled transformation of hemimicellar aggregates of dodecyl sulfate into a condensed monolayer at the Au(111) electrode surface, *Langmuir* **1999**, *15*, 2607–2616.

(5) Bizzotto, D.; Zamlynny, V.; Burgess, I.; Jeffrey, C. A.; Li, H.-Q.; Rubinstein, J.; Merril, R. A.; Lipkowski, J.; Galus, Z.; Nelson, A.; Pettinger, B. Amphiphilic and ionic surfactants at electrified interfaces, in: A. Wieckowski (Ed.), *Interfacial Electrochemistry*, Marcel Dekker, New York, **1999**, 405–426.

(6) Burgess, I.; Zamlynny, V.; Szymanski, G.; Lipkowski, J.; Majewski, J.; Smith, G.; Satija, S.; Ivkov, R. Electrochemical and neutron reflectivity characterization of dodecyl sulfate adsorption and aggregation at the gold-water interface, *Langmuir* **2001**, *17*, 3355–3367.

(7) Petri, M.; Kolb, D. M. Nanostructuring of a sodium dodecyl sulfate-covered Au (111) electrode, *Phys. Chem. Chem. Phys.* **2002**, *4*, 1211–1216.

(8) Chen, M.; Burgess, I.; Lipkowski, J. Potential controlled surface aggregation of surfactants at electrode surfaces – A molecular view, *Surf. Sci*. **2009**, *603*, 1878–1891.

(9) Leitch, J. J.; Collins, J.; Friedrich, A. K.; Stimming, U.; Dutcher, J. R.; Lipkowski, J. Infrared studies of the potential controlled adsorption of sodium dodecyl sulfate at the Au(111) electrode surface, *Langmuir* **2012**, *28*, 2455–2464.

(10) Sagara, T.; Izumi, K. Electroreflectance study of potential dependent phase changes of dodecyl sulfate adlayer on a Au(111) Electrode. *Electrochim. Acta* **2015**, 162, 4-10.

(11) Krause, C.; Mirsky, V. M.; Heckmann, K. D. Capacitive detection of surfactant adsorption on hydrophobized gold electrode, *Langmuir* **1996**, *12*, 6059.

(12) Hu, K.; Bard, A. J. Characterization of adsorption of sodium dodecyl sulfate on charge-regulated substrates by atomic force microscopy force measurements, *Langmuir* **1997**, *13*, 5418-5425.

(13) Cui, X.; Jiang, D.; Diao, P; Li, J.; Jia, Z.; Tong, R. Electrochemical studies for the formation of sodium lauryl sulfate monolayer on an octadecanethiol-coated gold electrode, *Colloids Surf., A* **2000**, *175*, 141-145.

(14) Bandyopadhyay, K.; Vijayamohanan, K.; Manna, A.; Kulkarni, B. D. Effect of co-adsorbed surfactant on the structure of self-assembled monolayer of thiol on polycrystalline gold, *J. Colloid Interface Sci.* **1998**, *206*, 224-230.

(15) Uosaki, K.; Sato, Y.; Kita, H. Electrochemical characteristics of a gold electrode modified with a self-assembled monolayer of ferrocenylalkanethiols, *Langmuir* **1991**, *7*, 1510-1514.

(16) Umeda, K.; Fukui, K. Observation of redox-state-dependent reversible local structural change of ferrocenyl-terminated molecular Island by electrochemical frequency modulation AFM, *Langmuir* **2010**, *26*, 9104-9110.

(17) Valincius, G.; Niaura G.; Kazakevičienė, B.; Talaikytė, Z.; Kažemėkaitė, M.; Butkus, E.; Razumas, V. Anion effect on mediated electron transfer through ferrocene-terminated self-assembled monolayers, *Langmuir* **2004**, *20*, 6631-6638.

(18) Yokota, Y.; Yamada, T.; Kawai, M. Ion-pair formation between ferrocene-terminated self-assembled monolayers and counteranions studied by force measurements, *J. Phys. Chem. C* **2011**, *115*, 6775-6781.

(19) Rudnev, A. V.; Yoshida, K.; Wandlowski, T. Electrochemical characterization of self-assembled ferrocene-terminated alkanethiol monolayers on low-index gold single crystal electrodes, *Electrochim. Acta* **2013**, *87*, 770-778.

(20) Kasuya, M.; Kurihara, K. Characterization of ferrocene-modified electrode using electrochemical surface forces apparatus, *Langmuir* **2014**, *30*, 7093-7097.

(21) Norman, L. L.; Badia, A. Electrochemical surface plasmon resonance investigation of dodecyl sulfate adsorption to electroactive self-assembled monolayers via ion-pairing interactions, *Langmuir* **2007**, *23*, 10198-10208.

(22) Dionne, E. R.; Badia, A. Electroactive self-assembled monolayers detect micelle formation, *ACS Appl. Mater. Interfaces*, **2017**, *9*, 5607-5621.

(23) Wade, J.; Leasor, C.; Chen, K.-H.; Hinkle, A.; Dailey, C. D.; Li, Z. Molecular imaging of viologen adlayers and in situ monitoring structural transformations at electrode–electrolyte interfaces, *ACS Sensors* **2021**, *6*, 493-501.

(24) Atherton, S. J.; Baxendale, J. H.; Hoey, B. M. Quenching of fluorescence from $Ru(dipy)^{2+}{}_3$ and $Ru(dipy)_2(CN)_2$ in solutions of sodium dodecyl sulphate, *J. Chem. Soc., Faraday Trans*. 1 **1982**, *78*, 2167-2181.

(25) Park, J. W.; Nam, H.-L. Association of methyl viologen and its cationic radical with sodium dodecyl sulfate, *Bull. Korean Chem. Soc.* **1984**, *5*, 182-187.

(26) Park, J. W.; Ko, S. H.; Park. J.-Y. Electrochemical studies of viologens in homogeneous aqueous and sodium dodecyl sulfate micellar solutions, *Bull. Korean Chem. Soc.* **1992**, *13*, 259-265.

(27) Engelman, E. E,; Evans, D. H. Treatment of the electrodeposition of alkyl sulfate salts of viologen radical cations as an equilibrium process governed by a solubility product, *Anal. Chem.* **1994**, *66*, 1530-1534.

(28) Monk, P. M. S. The Viologens, Wiley: Chichester, **1998**; p 17 and pp 186-187.

(29) Tominaga, T.; Ohtaka-Saiki, H.; Nogami, Y.; Iwata, H. Tracer diffusion of viologen dications in aqueous NaCl, KBr, NaDS, and DTABr solutions, *J. Mol. liq.* **2006**, *125*, 147-150.

(30) Tan, C.; Pinto, M. R.; Schanze, K. S. Photophysics, aggregation and amplified quenching of a water-soluble poly(phenylene ethynylene) *Chem. Commun.* **2002**, 446-447.

(31) Colaneri, M. J.; Kevan, L.; Thompson, D. H. P.; Hurst, J. K. Variation of alkymethylviologen radical cation-water interactions in micelles and vesicles from ESEM spectroscopy: Effect of alkyl chain length, *J. Phys. Chem*. **1987**, *91*, 4072-4077.

(32) McManus, H. J. D.; Kang, Y. S.; Kevan, L. Electron spin resonance, electron spin echo, and electron nuclear double resonance studies of the photoreduction yield of a series of alkylmethylviologens in sodium dodecyl sulfate and dodecyltrimethylammonium chloride micelles: effect of the alkyl chain length of the viologen, *J. Phys. Chem.* **1992**, *96*, 5622-5628.

(33) Hiley, S. L.; Buttry, D. A. Control of access to surfaces with self-assembling surfactants bearing fluorocarbon chains, *Colloid Surf. A-Physicochem. Eng. Asp.* **1994**, *84*, 129-140.

(34) Sagara, T.; Tsuruta, H.; Nakashima, N. Does thiol-functionalized viologen monolayer memorize anion present when forming the monolayer?, *J. Electroanal. Chem.* ***2001***, *500*, 255-263.

(35) De Long, H. C.; Buttry, D. A. Environmental effects on redox potentials of viologen groups embedded in electroactive self-assembled monolayers, *Langmuir* **1992**, *8*, 2491-2496.

(36) Li, Z.; Han, B.; Meszaros, G.; Pobelov, I.; Wandlowski, T.; Blaszczyk, A.; Mayor, M. Two-dimensional assembly and local redox-activity of molecular hybrid structures in an electrochemical environment, *Faraday Discuss.* **2006**, *131*, 121-143.

(37) Han, B.; Li, Z.; Wandlowski, T.; Blaszczyk, A.; Mayor, M. Potential-induced redox switching in viologen self-assembled monolayers: an ATR-SEIRAS approach, *J. Phys. Chem. C*, **2007**, *111*, 13855-13863.

(38) Liu, B.; Blaszczyk A.; Mayor, M.; Wandlowski, T. Redox-switching in a viologen-type adlayer: an electrochemical shell-Isolated nanoparticle enhanced Raman spectroscopy study on Au(111)-(1 X 1) single crystal electrodes, *ACS Nano* **2011**, *5*, 5662-5672.

(39) Wen, B.-Y.; Lin, J.-S.; Zhang, Y.-J.; Radjenovic, P. M.; Zhang, X.-G.; Tian, Z.-Q.; Li; J.-F. Probing electric field distributions in the double layer of a single-crystal electrode with angstrom spatial resolution using Raman spectroscopy, *J. Am. Chem. Soc.* **2020**, *142*, 11698–11702.

(40) Sagara, T.; Kaba, N.; Komatsu, M.; Uchida, M.; Nakashima, N. Estimation of average orientation of surface-confined chromophores on electrode surfaces using electroreflectance spectroscopy, *Electrochim. Acta* **1998**, 43, 2183-2193.

(41) Sagara, T.; Maeda, H.; Yuan, Y.; Nakashima, N. Voltammetric and electroreflectance study of thiol-functionalized viologen monolayers on polycrystalline gold: Effect of anion binding to a viologen moiety, *Langmuir* **1999**, *15*, 3823-3830.

(42) Sagara, T. UV-visible reflectance spectroscopy of thin organic films at electrode surfaces, in: Alkire, C.; Kolb, D. M.; J. Lipkowski, J.; Ross, P. N. (Eds.), Advances in Electrochemical Science and Engineering, Vol. 9, Wiley-VCH Verlag, Weinheim, **2006**, pp 47–95.

(43) Riddick J. A.; Bunger W. B. Organic solvents: physical properties and methods of purification, third edition, Wiley, New York, **1970**.

(44) Traube, J. Über die Capillaritatsconstanten organischer Stoffe in wässerigen Lösungen, *Ann*., **1891**, *265*, 27-55.

(45) Langmuir, I. The constitution and fundamental properties of solids and liquids. II. liquids, *J. Am. Chem. Soc.* **1917**, *39*, 1848-1906.

(46) Adamson, A. W. *Physical Chemistry of Surfaces*, 5th ed.; Wiley: New York, **1990**.

(47) Fujimoto, K.; Yoshii, N.; Okazaki, S. Molecular dynamics study of solubilization of immiscible solutes by a micelle: Free energy of transfer of alkanes from water to the micelle core by thermodynamic integration method, *J. Chem. Phys.* **2010**, *133*, 074511.

(48) Wishnia, A. The hydrophobic contribution to micelle formation: the solubility of ethane, propane, butane, and pentane in sodium dodecyl sulfate solution, *J. Phys. Chem.* **1963**, *67*, 2079-2082.

(49) Tian, H.; Dai, Y.; Shao, H.;Yu H.-Z. Modulated intermolecular interactions in ferrocenylalkanethiolate self-assembled monolayers on gold, *J. Phys. Chem. C* **2013**, *117*, 1006–1012.

(50) Bizzotto, D.; Burgess, I.; Doneux, T.; Sagara, T.; Yu H.-Z. Beyond simple cartoons: Challenges in characterizing electrochemical biosensor interfaces, *ACS Sens.* **2018**, *3*, 5–12.

Authors are required to submit a graphic entry for the Table of Contents (TOC) that, in conjunction with the manuscript title, should give the reader a representative idea of one of the following: A key structure, reaction, equation, concept, or theorem, etc., that is discussed in the manuscript. Consult the journal's Instructions for Authors for TOC graphic specifications.

Insert Table of Contents artwork here

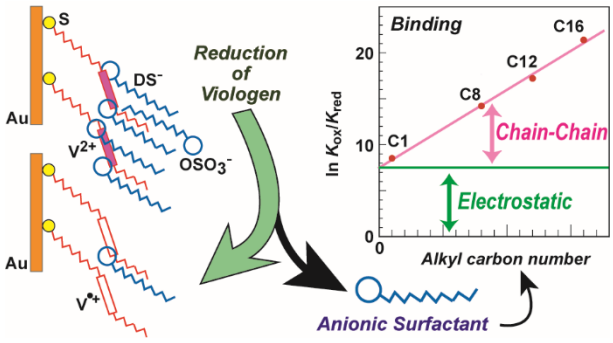

Supporting Information

Binding of Sulfate-Terminated Surfactants with Different Alkyl Chain Lengths to Viologen Sites Covalently Embedded in the Interior of a Self-Assembled Monolayer on a Au Electrode

Takamasa Sagara*,†, Youichi Hagi‡, Masaki Toyohara§

† Division of Chemistry and Materials Science, Graduate School of Engineering, Nagasaki University, Nagasaki, Nagasaki 852-8121, Japan

‡ Department of Materials Engineering and Molecular Science, Graduate School of Science and Technology, Nagasaki University, Bunkyo 1-14, Nagasaki 852-8521, Japan

§ Department of Advanced Technology and Science for Sustainable Development, Graduate School of Engineering, Nagasaki University, Nagasaki, 852-8521, Japan

Table of Contents

Table S1. Results of XPS elemental analysis

Sample	Elemental ratio (calculated)	Elemental ratio (obtained)[a)]
C7VC10-SH(PF_6^-)$_2$ monolayer on Au, as prepared	**S = 1, N = 2, P = 2** **F = 12**	**S = 1.00, N = 3.43, P = 2.34** **F = 9.63, C = 171.5**
C7VC10-SH monolayer on Au, after multiple CV scan in KF solution	**S = 1, N = 2, P = 0** **F = 2**	**S = 1.00, N = 2.04, P = 0.00** **F = 0.514, C = 114**
C7VC10-SH monolayer on Au, after multiple CV scan in 300 μM SDS solution (base solution of KF)	**S = 3 (Assuming 1:2 Binding of DS-)** **N = 2** **F = residual from electrolyte**	**S = 3.00** **N = 6.94 (N/S = 2.31)** **F = 2.54, C = 471**

a) ESCA mode measurements were conducted to detect integrated intensity normalized to S at the peaks of F(1s) at 686.30 eV, C(1s) at 284.75 eV, N(1s) at 402.10 eV, P(2p) at 136.10 eV S(2p) at 162.80 eV. Because the small angle incidence was not used, the escape-depths of the atoms were not considered.

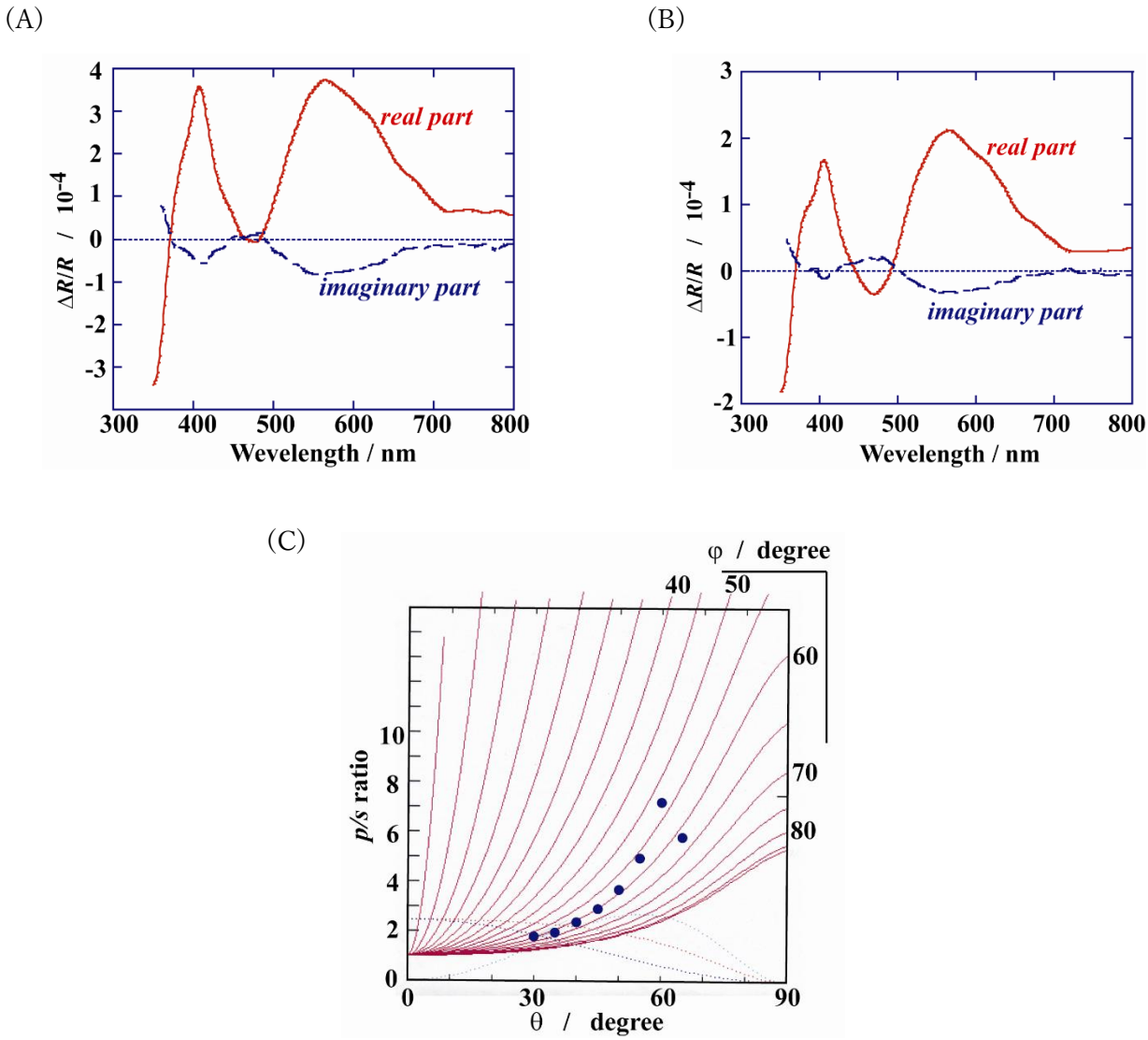

Figure S1. Results of electroreflectance (ER) measurements.

For the measurement parameters, refer to Eq. (1) in the paper.

(A) and (B) are ER spectra with 45° incidence of non-polarized light with E_{dc} adjusted to be equal to the formal potentials, f = 14 Hz, and ΔE_{ac} = 50 mV_{rms}). (A) was obtained in 0.1 M KF solution and (B) in 0.1 M KF solution + 0.1 mM SDS solution. (C) is the plot of p/s ratio of ER signal with polarized light (p and s polarization) incidence at 602 nm as a function of incident angle (θ) obtained in 0.1 M KF solution + 0.1 mM SDS solution. Thin red lines represent simulated working curves. The data points were in line with an orientation angle (φ) of 60° for the longitudinal axis of viologen radical cation with respect to the surface normal. Note that the orientation angle was in the range of 60°-65° regardless of the anionic species in the solution.

For details of ER measurements: Sagara, T. In *Advances in Electrochemical Science and Engineering, Volume X: In situ Spectroscopic and Diffraction Methods*, Alkire, C.; Kolb, D. M.; Lipkowski, J.; Ross, P. N. Eds.; Wiley-VCH Verlag, GmbH, Weinheim, 2006, pp 47-95.)